

Absolute cross sections for H^+ formation from electron-impact dissociation of C_2H^+ and $C_2H_2^+$

D. B. Popović,¹ N. Djurić,¹ K. Holmberg,² A. Neau,² and G. H. Dunn¹

¹*JILA, University of Colorado and National Institute of Standards and Technology, Boulder, Colorado 80309-0440*

²*Department of Physics, Stockholm University, Box 6730, S-113 85 Stockholm, Sweden*

(Received 10 April 2001; published 5 October 2001)

Absolute cross sections as a function of interaction energy were measured for H^+ formation in electron-impact dissociation of C_2H^+ and $C_2H_2^+$ in the energy range from threshold up to 50 eV. The crossed beams technique was used, and light fragment ions emerging from a heavy target were detected. A common feature of the studied targets was almost the same $[(1.3-1.7) \times 10^{-16} \text{ cm}^2]$ cross section for H^+ production from 25 to 50 eV. The results were compared with our previous results for CD_n^+ , and the observed propensity rules were found to apply in this case also.

DOI: 10.1103/PhysRevA.64.052709

PACS number(s): 34.80.Gs, 34.80.Kw

I. INTRODUCTION

Hydrocarbon ions are present in a number of different media including flames [1], industrial plasmas [2], thermonuclear reactor divertors [3], and astrophysical objects such as the ionospheres of Jupiter [4] and Titan [5] and dense interstellar clouds [6]. About 10% of the molecules that have been identified in the interstellar clouds are actually molecular ions [7], and those containing carbon are the most abundant [7]. The acetylene ion $C_2H_2^+$ plays an important role in space and in laboratory chemistry [8]. Both the acetylene molecule and its radical cation are of great importance to fundamental research; they are small enough to be treated by theories and large enough to be model cases for molecular dynamic processes [9].

Information on light hydrocarbons is needed for modeling fusion edge plasmas. Fusion plasma devices often use graphite as the material for inner walls in order to reduce radiation losses [10,11], so hydrocarbons are produced at these walls.

Electron-impact dissociative excitation, ionization, and recombination of simple hydrocarbons are processes important for modeling of plasmas. Dissociative recombination is the most studied among these [12,13]. Dissociative excitation (DE), which is the subject of this paper, has been less studied, and dissociative ionization (DI) studied even less than that [13].

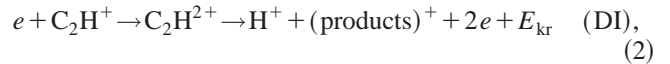
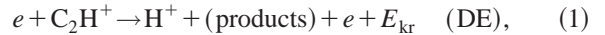
Our experiment is configured to detect light fragment ions (H^+ or D^+) formed in electron-impact dissociation of molecular ions. There are technical difficulties in detecting and measuring light fragment ions from electron-impact dissociation of molecular ion parents, since the hydrogen is so much lighter than the parent or any other product. To conserve momentum, it carries away essentially all of the excess energy, and thus it comes out at large angles and with a broad laboratory energy spread, which makes it difficult to collect and detect. We have previously reported [14–16] dissociation cross sections for D^+ and D_2^+ formation from CD_n^+ , ND_n^+ , and OD_n^+ ions. We found that the D^+ formation channel is dominant with the associated cross sections being independent of the number of D atoms in the target; i.e., the cross sections for D^+ production from all the target ions investigated rise to similar magnitudes. Results obtained for

C_2H^+ and $C_2H_2^+$ are presented in this article. We note that to our knowledge neither experimental nor theoretical results have been previously obtained for the DE or DI processes involving these ions.

II. EXPERIMENTAL TECHNIQUE

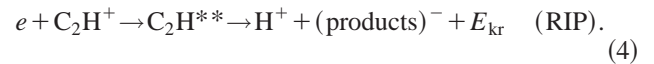
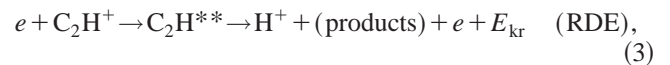
A. General concepts

When an electron collides with a molecular ion, different processes may occur depending on the electron energy. Since we are detecting light positively charged ions, we focus on the following *direct* processes that lead, in the case of C_2H^+ , to H^+ production:



where E_{kr} stands for kinetic energy release.

Other, *indirect* processes also contribute to H^+ formation. They proceed via resonant capture of an electron by the ion into doubly excited neutral states. These doubly excited states can stabilize via autoionization or they can dissociate through different channels. The ones interesting to us, which lead to formation of ionic fragments, are resonant dissociative excitation (RDE) and resonant ion pair (RIP) formation:



The H^+ products from all four of these processes may be detected in our measurements.

A crossed electron-ion beams configuration was used to measure the absolute dissociation cross section σ for formation of H^+ ions. The cross section at each energy E was calculated [17] from measured quantities using the relationship

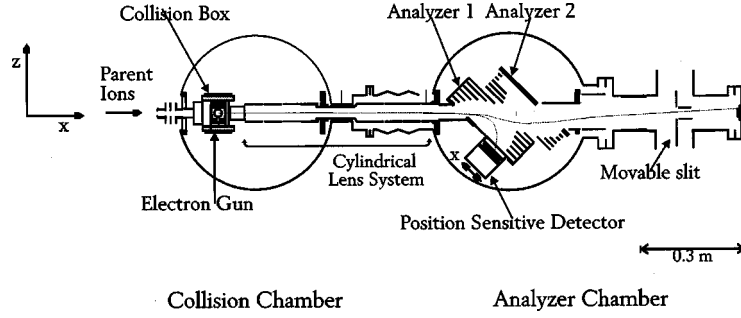


FIG. 1. Once the positive ions are formed and mass selected, they enter the collision chamber where they collide with the electron beam (at 90°). The product fragment ions (H^+) and the parent ions ($C_2H_2^+$ or C_2H^+) are then transported via a cylindrical lens system to the analyzer chamber where the first 45° electrostatic analyzer separates the fragment ions from the parent ions and deflects them onto a position-sensitive detector (PSD), and the second 45° electrostatic analyzer redirects the parent ions to an electrically isolated small chamber where the parent ion current is measured.

$$\sigma(E) = \frac{e^2 R}{I_e I_i \varepsilon} \left[\frac{v_e v_i}{\sqrt{v_e^2 + v_i^2}} \right] F, \quad (5)$$

where e is the elementary unit of charge; R is the H^+ fragment ion signal count rate; v_e and v_i are laboratory velocities of electrons and ions; I_e and I_i are electron and ion currents; ε is the efficiency for collection and detection of H^+ fragment ions; and F is the form factor, which gives a measure of the overlap between the electron and ion beams [17].

B. Apparatus

The experimental apparatus is shown in Fig. 1. Ions are produced in a commercial hot-cathode discharge ion source [18]. Neutral gas (a mixture of C_2H_2 and He in the present case) is fed into this source, where ions are produced with an unknown distribution of internal states. There is no possibility of controlling the internal states of the target ions. Hence, if the ions are produced in excited states, with lifetimes longer than the $10 \mu\text{sec}$ transit time to the collision region, the appearance potential of H^+ is lower than in the case of the parent ion's being in the ground state. Ions are extracted through a hole in the anode, accelerated (typically to energies of 5000–7000 eV), and led to a 60° sector magnetic-field analyzer that separates them according to their m/q ratio. Since $C_2H_2^+$ ions have the same mass as CN^+ ions, special care was taken to eliminate nitrogen from the gas line and ion source of our system. This is important because otherwise both of these ions would contribute to the target ion current. Ions of a chosen mass are then transported into a collision box (inside the collision chamber) where they collide at 90° with a magnetically confined (0.006 T) electron beam [19]. To determine the beam overlap, a scanning (rotatable) slit probe is moved into and out of the center of the collision box to measure the profiles of both the electron and ion beams. After electron-impact dissociation, both the target and fragment ions enter a cylindrical lens system that accelerates and transports them to the analyzer chamber. This cylindrical lens system consists of five cylinders at different voltages, followed by a tube and then another three cylinders; some of the cylinders are cut so that they can be used as vertical and horizontal deflectors for the ions.

A three-dimensional trajectory modeling program [20] was used to optimize the capability of the ion optical system to transport relevant fragments and collect them and also to separate them from the parent ion beam and from other fragments.

The analyzer chamber consists of two 45° electrostatic analyzers. The first analyzer selects the fragment ions of interest and deflects them to a position-sensitive detector (PSD) that consists of two microchannel plates (with a diameter of 40 mm) backed by a resistive anode. The detector is mounted on a linear motion feedthrough with a 50 mm linear range of motion. Since the parent ion beam is slightly deflected by the first analyzer, we redirect it toward an electrically isolated smaller chamber using a second analyzer and the horizontal deflectors that follow. This smaller chamber is used as a large ion collector and serves for measuring the parent ion current.

Light ion products of dissociation are particularly difficult to detect because, as kinematic arguments show [14], they take almost all of the kinetic energy release upon dissociation and fly off in a wide range of angles, and with a broad energy spread. Therefore, special care was taken to configure the apparatus so that it collects the ions scattered within these wide ranges of angles and energies. There is usually no single position of the movable PSD that can collect all of them. Therefore, data were taken at each electron energy at several PSD positions and the results at that energy summed to obtain the final result. However, this detector motion does not accommodate possible loss of particles in the vertical direction. Our simulations using the trajectory modeling program [20] show that we are collecting all the ions with E_{kr} of 7 eV or less. This means that if $E_{kr} > 7$ eV it is possible that not all of the fragment ions are detected, and that the true cross section may be greater than that measured.

The PSD efficiency ε for detection of H^+ ions in the present case is taken to be 0.24 ± 0.05 , taking into account our previous efficiency measurements [14] and energy dependence [21] measurements of ε .

Fragment ions are also produced by ion collisions with both residual gas and surfaces. These background signals are often much larger than the signal of interest. Therefore, the electron beam was chopped (at 1000 Hz) to alternately ob-

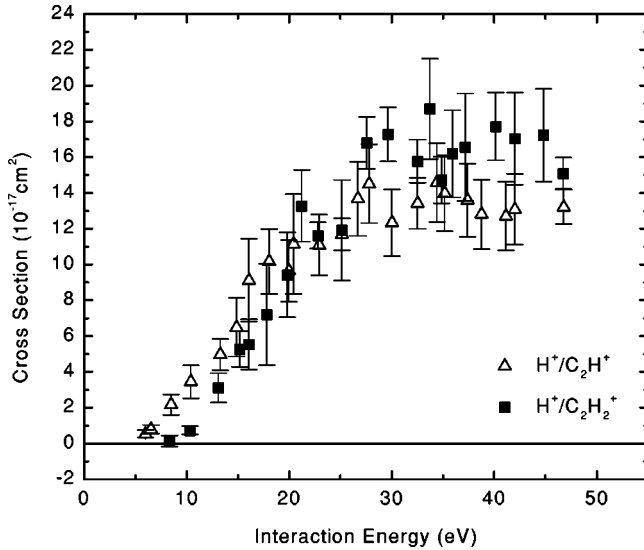


FIG. 2. Absolute cross sections for production of H⁺ fragment ions in electron-C₂H₂⁺ and electron-C₂H⁺ collisions, as a function of interaction energy. Points represent average experimental values, and bars characterize the relative uncertainties at one standard deviation (1σ) level.

tain the signal plus background and the background alone. The difference between these two gives the true signal.

III. RESULTS AND DISCUSSION

A. General behavior of experimental cross sections

The absolute cross sections for H⁺ ion fragment formation in electron collisions with C₂H⁺ and C₂H₂⁺ ions are shown in Fig. 2. As seen, these cross sections are almost identical. After a slow rise from the threshold at around 5 eV for C₂H⁺ and 8 eV for C₂H₂⁺ ions, the maximum [(1.3–1.7) × 10⁻¹⁶ cm²] is reached at about 30 eV, and the cross sections remain near that value for all the higher energies at which the measurements were performed.

Similar cross section behavior was observed in our earlier studies [15] of D⁺ formed from electron collisions with hydrocarbon ions CD_n⁺ (n=2 to 5), as well as in the cases [16] of ND_n⁺ (n=2 to 4) and OD_n⁺ (n=2,3). The results for CD_n⁺ are reproduced in Fig. 3 for comparison.

B. Results for C₂H⁺

It can be seen in Fig. 2 that the measured appearance of H⁺ ions is about 5 eV. It is difficult to state the energy at which H⁺ is expected to first appear. The proton affinity for C₂ is calculated [22] to be 4.4 eV. As far as we know, there is no information about repulsive surfaces to which transitions are made in order to yield H⁺. If one assumes vertical transitions, the proton affinity plus some unknown energy necessary to reach the repulsive surface should be the appearance energy of H⁺ from cold C₂H⁺. Since these repulsive surfaces are not known, no comparisons can be made with expected and observed appearance energies. The fact that the cross section is nonzero at energies only slightly higher than the proton affinity leads us to assume that we

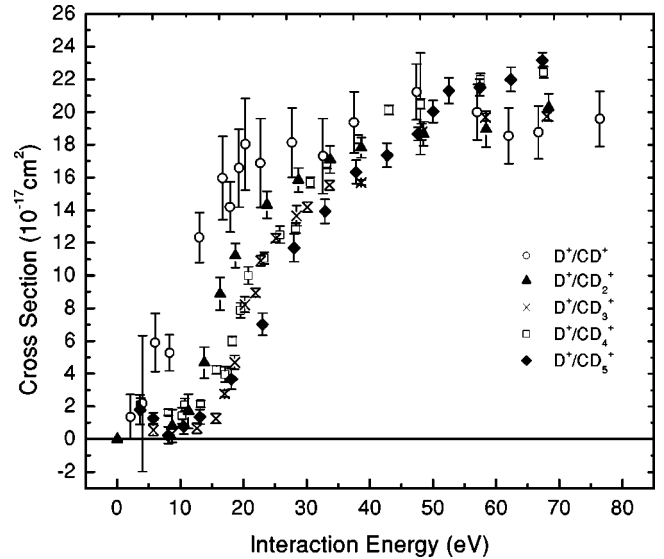
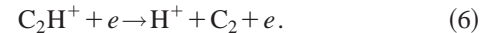
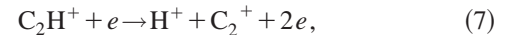


FIG. 3. Absolute cross sections, as a function of interaction energy, for production of D⁺ ions in electron collisions with CD_n⁺ [15]. Points represent averaged experimental values, and bars display relative uncertainties at 1σ level.

probably have internally excited parent ions. However, one should not neglect the RDE process which could also contribute to the appearance of the H⁺ signal in the energy range between the proton affinity and the minimum energy for vertical transition required for direct DE. Furthermore, there could be some contributions from RIP and since C₂ has electron affinity of 3.3 eV [23] this would place the appearance potential for H⁺ at 1.13 eV. The most likely process responsible for the rise in signal at 5 eV is simply



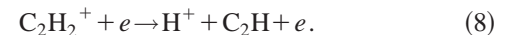
One observes a change in the slope in Fig. 2 at the energy of about 17 eV, and this can probably be attributed to the DI process



which has a minimum required energy of 15.8 eV.

C. Results for C₂H₂⁺

The minimum energy required for appearance of H⁺ in the case of C₂H₂⁺ is the proton affinity of C₂H, which is reported as 7.80 eV [23], plus some unknown energy necessary for the electron to reach the repulsive surface:



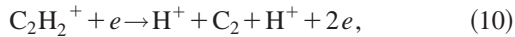
It can be seen in Fig. 2 that the energy at which we begin to see the H⁺ signal is approximately equal to the proton affinity. Again, as in the case of H⁺ from C₂H⁺, one must keep in mind that the parent ions may be internally excited, and there may be contributions from RDE and RIP.

The number of processes contributing to H⁺ production is even larger than in the case of C₂H⁺. One observes changes in the slope in the curve representing the H⁺ signal from

$C_2H_2^+$ in Fig. 2 at approximately 21 eV and 28 eV. The process that could lead to an increase in H^+ production near the lower energy could be DI at 19.38 eV:



The process leading to increase of H^+ production near 28 eV could be



which has the minimum energy required for it to take place of 27.75 eV.

D. Uncertainties

Relative uncertainties in our measurements, shown in Fig. 2 by the bars, are due to counting statistics, uncertainties in the form factor, and uncertainties in the procedure for summing up the signal at different PSD positions. These relative uncertainties are combined to obtain the total relative uncertainty at one standard deviation (1σ) level [24]. In addition, there are systematic uncertainties that do not affect the relative shape of the cross section curve. Thus the total absolute uncertainty is obtained by adding in quadrature the systematic uncertainty to the relative uncertainty and it is estimated to be $\pm 25\%$ at the 1σ level for points near the maximum cross section.

E. Propensity rules

The measurements reported here are consistent with the propensity rules we have previously articulated [14–16] and which we repeat here.

(1) The cross section magnitudes for obtaining $H^+(D^+)$ ions are independent of the number n of H (D) atoms in the target ion.

(2) These cross sections all rise to very similar values [$(1.3\text{--}2) \times 10^{-16} \text{ cm}^2$] and remain independent of energy after reaching this maximum up to 50 eV.

(3) Dissociation cross sections to produce D_2^+ fragments are about an order of magnitude smaller than those for D^+ production from CD_n^+ , ND_n^+ , and OD_n^+ . Although the H_2^+

channel was not investigated here, we would anticipate on the basis of this rule that it will be about an order of magnitude smaller than found here for H^+ . Of course, this remains to be investigated.

No explanations have been put forth for the fact that the cross sections for the different targets, despite these targets having different threshold energies and different numbers of H (D) atoms, rise finally to almost the same value and remain relatively flat over the energy range investigated.

We are not aware of any other measurements of dissociative excitation and dissociative ionization performed on C_2H^+ and $C_2H_2^+$ ions.

IV. CONCLUSION

We report here the results of cross section measurements for electron-impact dissociation of C_2H^+ and $C_2H_2^+$ in the energy range between 5 and 50 eV. The total expanded uncertainty in the results is about $\pm 25\%$. The technique that we have employed is specifically for measuring light fragment ions formed from breakup of small molecular ions. These measurements are a continuation of our earlier studies of dissociation of molecular ions containing hydrogen. We observe the same propensity rules as in our earlier investigations [14–16]: the cross sections for obtaining H^+ ions are independent of the number n of H atoms in the target ion and they all rise to very similar magnitudes [$(1.3\text{--}1.7) \times 10^{-16} \text{ cm}^2$] and remain independent of energy after reaching this maximum.

The present measurements for C_2H^+ and $C_2H_2^+$ are not compared with other measurements or theory since such data are apparently nonexistent.

ACKNOWLEDGMENTS

This work was supported in part by the Office of Fusion Energy of the U. S. Department of Energy under Contract No. DE-A102-95ER54293 with the National Institute of Standards and Technology. This work was also supported by the Swedish Foundation for International Cooperation in Research and Higher Education.

-
- [1] A. N. Hayhurst and H. R. N. Jones, *J. Chem. Soc., Faraday Trans. 2* **83**, 1 (1987).
- [2] D. C. Schram, D. K. Otorbaev, R. F. G. Meulenbroeks, M. C. M. van de Sanden, M. J. J. Eerden, and J. A. M. van der Mullen, in *Dissociative Recombination: Theory, Experiment and Applications III*, edited by D. Zajfman, J. B. A. Mitchell, D. Schwalm, and B. R. Rowe (World Scientific, Singapore, 1996), p. 29.
- [3] H. Tawara, in *Atomic and Molecular Processes in Fusion Edge Plasmas*, edited by R. K. Janev (Plenum, New York, 1995), p. 461.
- [4] Y. H. Kim and J. L. Fox, *Icarus* **112**, 310 (1994).
- [5] J. L. Fox, in *Dissociative Recombination: Theory, Experiment and Applications III* (Ref. [2]) p. 40.
- [6] E. Herbst, *Annu. Rev. Phys. Chem.* **46**, 27 (1995).
- [7] A. M. Derkatch, A. Al-Khalili, L. Viktor, A. Neau, W. Shi, H. Danared, M. af Ugglas, and M. Larsson, *J. Phys. B* **32**, 3391 (1999).
- [8] M.-F. Jagod, M. Rosslein, C. M. Gabrys, B. D. Rehfuss, F. Scappini, M. W. Crofton, and T. Oka, *J. Chem. Phys.* **97**, 7111 (1992).
- [9] Ch. Cha, R. Weinkauff, and U. Boesl, *J. Chem. Phys.* **103**, 5224 (1995).
- [10] H. Tawara, T. Tonuma, H. Kumagai, and T. Matsuo, *J. Phys. B* **25**, L423 (1992).
- [11] H. Tawara and R. A. Phaneuf, *Comments At. Mol. Phys.* **22**, 963 (1988).
- [12] M. Larsson, in *Photoionization and Photodetachment*, Vol. 10

- of *Advanced Series in Physical Chemistry*, edited by C.-Y. Ng (World Scientific, Singapore, 2000), p. 693.
- [13] G. H. Dunn and N. Djurić, in *Novel Aspects of Electron-Molecule Scattering*, edited by K. Becker (World Scientific, Singapore, 1998), p. 241.
- [14] N. Djurić, Y.-S. Chung, B. Wallbank, and G. H. Dunn, *Phys. Rev. A* **56**, 2887 (1997).
- [15] N. Djurić, S. Zhou, G. H. Dunn, and M. E. Bannister, *Phys. Rev. A* **58**, 304 (1998).
- [16] N. Djurić, A. Neau, S. Rosen, W. Zong, and G. H. Dunn, *Phys. Rev. A* **62**, 032702 (2000).
- [17] G. H. Dunn, in *Electron Impact Ionization*, edited by T. D. Märk and G. H. Dunn (Springer-Verlag, Vienna, 1985), p. 277.
- [18] M. Menzinger and L. Wahlin, *Rev. Sci. Instrum.* **40**, 102 (1969).
- [19] P. O. Taylor, K. T. Dolder, W. E. Kauppila, and G. H. Dunn, *Rev. Sci. Instrum.* **45**, 538 (1974).
- [20] D. A. Dahl, *Computer code SIMION 3D*, Version 6.0, Idaho National Engineering Laboratory.
- [21] R. S. Gao, P. S. Gibner, J. H. Newman, K. A. Smith, and R. F. Stebbings, *Rev. Sci. Instrum.* **55**, 1756 (1984).
- [22] W. A. Lathan, W. J. Hehre, and J. A. Pople, *J. Am. Chem. Soc.* **93**, 808 (1971).
- [23] *NIST Chemistry WebBook*, Natl. Inst. Stand. Technol. Standard Reference Database No. 69, edited by W. G. Mallard and P. J. Linstrom (National Institute of Standards and Technology, Gaithersburg, 2000).
- [24] B. N. Taylor and C. E. Kuyatt, NIST Technical Report No. 1297, 1993 (unpublished).